BIOSCIENCES BIOTECHNOLOGY RESEARCH ASIA, September 2026. Vol. **23**(3), p. 1277-1288

Integrated In Silico Investigation of Imidazolidine Derivatives Targeting NUDT5 (PDB ID: 7B6F): Molecular Docking, ADMET, and Drug-Likeness Assessment

Harshada Subhash Bhosale[1], Rohit Jaysing Bhor[1]*, Ashok Yuvraj Dalimbe[2], Sachin Dattatraya Nawale[2], Pranali Satish Pandarkar[2], Divya Ravindra Shivtare[2] and Aditya Anil Pachpute[2]

[1]Department of Pharmaceutical Chemistry, Pravara Rural College of Pharmacy, Ahmednagar, India.
[2]Department of Pharmaceutical Chemistry, H.S.B.P.V.T's GOI. Faculty of Pharmacy, Ahilyanagar, India.

http://dx.doi.org/10.13005/bbra/3571

(Received: 14 April 2026; accepted: 29 August 2026)

Ovarian cancer remains a major global health challenge, highlighting the need for the discovery of novel therapeutic agents targeting cancer-associated molecular pathways. The present study aimed to design and computationally evaluate a series of imidazolidine derivatives (AM1–AM12) as potential inhibitors of the ovarian cancer-associated target protein 7B6F. The designed compounds were subjected to an integrated in silico evaluation comprising molecular docking, physicochemical property analysis, drug-likeness assessment, ADMET prediction, and protein–ligand interaction analysis. Molecular docking was performed to estimate the binding affinity of the designed derivatives toward the target protein. The compounds exhibited docking scores ranging from "7.1 to "9.9 kcal/mol, indicating favorable binding interactions. Among the evaluated derivatives, AM8, AM9, AM6, and AM7 showed the strongest binding affinities, with their binding modes supported by hydrogen-bonding, hydrophobic, and electrostatic interactions with key amino acid residues within the target binding site. Physicochemical profiling demonstrated that most derivatives possessed acceptable molecular weight, lipophilicity, hydrogen-bonding capacity, and molecular flexibility. ADMET prediction indicated high gastrointestinal absorption for all evaluated compounds, although variations in other pharmacokinetic parameters were observed among the derivatives. Drug-likeness analysis further showed that most compounds complied with established Lipinski, Veber, and Egan criteria, with minimal rule violations. Based on the combined docking, ADMET, physicochemical, and drug-likeness profiles, AM7, AM8, and AM9 were identified as the most promising candidates. Overall, the integrated computational findings suggest that these imidazolidine derivatives may serve as potential lead molecules for ovarian cancer drug discovery and warrant further molecular optimization and experimental validation to confirm their anticancer activity.

Keywords: ADMET profiling, Drug-likeness, Molecular docking, Ovarian cancer, Pharmacokinetics, Structure-based drug design.

Ovarian cancer remains one of the most frequently diagnosed malignancies in women worldwide and constitutes a significant global health burden due to its high incidence and mortality rates. It originates from the abnormal and uncontrolled proliferation of epithelial cells within ovarian tissue,[1] commonly arising from the surface epithelium. Molecular biomarkers

*Corresponding author E-mail: rohit.bhor69@gmail.com

This is an Open Access article licensed under a Creative Commons license: Attribution 4.0 International (CC-BY).
Published by Oriental Scientific Publishing Company © 2026

such as estrogen receptor (ER),[2] progesterone receptor (PR),[3] and human epidermal growth factor receptor 2 (HER2),[4] play a crucial role in disease classification,[5] prognosis, and the development of targeted therapies. Despite considerable progress in diagnostic techniques and therapeutic interventions,[6] the effective management of ovarian cancer is still limited by factors such as tumor metastasis,[7] recurrence, and the emergence of drug resistance. In this context,[8] structure-based drug design has gained prominence as a rational and efficient strategy for the discovery of novel anticancer agents. This approach focuses on the identification and structural characterization of specific biomolecular targets involved in tumor progression. The protein structure available in the Protein Data Bank under PDB ID: 7B6F has recently attracted interest as a promising target for computational drug discovery. Proteins of this class are typically involved in enzymatic or regulatory mechanisms that govern essential cellular functions,[9] including cell proliferation, programmed cell death (apoptosis), and metabolic homeostasis, which are often dysregulated in cancerous conditions. The well-resolved three-dimensional architecture of the 7B6F protein, along with its defined active binding pocket,[10] makes it highly suitable for molecular docking and ligand interaction studies. The binding cavity of this protein comprises critical amino acid residues capable of establishing hydrogen bonding,[11] hydrophobic contacts, and electrostatic interactions with candidate ligands. These molecular interactions play a pivotal role in stabilizing protein–ligand complexes and directly influence binding affinity and specificity. Therefore, evaluating the interaction patterns between small molecules and the 7B6F protein can provide valuable insights into the rational design of potent inhibitory compounds with anticancer potential. Targeting proteins involved in tumor growth and survival signaling pathways represents a promising therapeutic approach in ovarian cancer treatment. Proteins structurally or functionally analogous to 7B6F are often associated with key oncogenic pathways,[12] including PI3K/AKT signaling,[13] MAPK cascades,[14] and apoptosis regulation. Modulation or inhibition of these pathways can effectively suppress tumor cell proliferation,[15] induce apoptotic cell death, and limit metastatic progression. In this regard, molecular docking studies employing the 7B6F protein serve as an essential preliminary step for the identification of potential lead compounds. The present investigation emphasizes the in silico assessment of synthesized compounds through docking analysis against the 7B6F protein. By evaluating parameters such as binding affinity,[16] interaction profiles,[17] and physicochemical characteristics,[18] this study aims to identify promising lead molecules with potential anticancer activity. Furthermore, proteins selected from structural databases like the Protein Data Bank, including 7B6F, are often implicated in diverse biological processes relevant to cancer progression, such as cellular proliferation, survival signaling, apoptotic pathways, inflammatory responses,[19] and enzyme-mediated metabolic regulation. If the 7B6F protein is functionally associated with oncogenic enzymes or signaling mediators, its inhibition could contribute to the suppression of tumor growth. Molecular docking investigations, such as those conducted with AM-series derivatives, provide valuable insights into the binding efficiency and inhibitory potential of these compounds, thereby facilitating the identification of novel therapeutic candidates for ovarian cancer management.

MATERIALS AND METHODS

Materials

The link between the target receptor, the anticipated lead chemical molecule,[20] and its protein receptors is often investigated using docking in modern drug research. The study was conducted electronically using computational techniques. ADMET Prediction in Silico to forecast their pharmacokinetic profiles,[21] the best medications selected from molecular docking studies were evaluated for ADME characteristics. The sketch tool in Discovery Studio is used to create the molecules in two and three dimensions. The compound was created in Marvin Sketch, optimized in three dimensions, and saved in SDF format.

Methods

Protein Preparation

The 7B6F Protein: Structural and Functional Insights

The 7B6F protein refers to a protein

structure available in the Protein Data Bank (PDB ID: 7B6F) given in figure 1, which is associated with enzymatic or regulatory roles depending on its biological context. Proteins like 7B6F are often investigated in structure-based drug design due to their defined three-dimensional conformations and potential involvement in disease-related pathways. Although the exact biological function of the 7B6F protein depends on its annotation,[22] it typically represents a targetable macromolecule whose active site can accommodate small-molecule ligands. Such proteins are frequently used in molecular docking studies to evaluate binding affinity and interaction mechanisms of novel compounds.

Protein Preparation of 7B6F for Molecular Docking in Ovarian Cancer Studies

Protein preparation is a critical step in structure-based drug design. The three-dimensional structure of the target protein (PDB ID: 7B6F) must be optimized to reflect its biologically active form prior to ligand interaction studies. Improper preparation can lead to inaccurate binding predictions and misinterpretation of results. Following structure cleaning, missing hydrogen atoms were added to the protein to correctly represent protonation states under physiological conditions. This step is essential for accurate modeling of hydrogen bonding and electrostatic interactions during docking. The protonation of residues such as lysine,[23] arginine,[24] aspartic acids,[25] and glutamic acid were assigned based on physiological pH (~7.4). Subsequently, the protein structure was subjected to energy minimization to relieve steric clashes and optimize bond geometries. This process ensures that the protein adopts a stable conformation suitable for docking analysis. Force fields such as OPLS or AMBER are commonly employed for this purpose. The prepared protein was then analyzed to identify the active binding site. This was achieved either by selecting the coordinates of the co-crystallized ligand binding pocket or by using computational tools for binding site prediction. Key amino acid residues, including LYS36, VAL37, THR38, THR39, VAL40, and ARG50, were identified as part of the active site region based on structural and docking studies. Finally, a grid box was generated around the active site to define the docking region. The grid dimensions were carefully chosen to encompass all critical residues involved in ligand binding while avoiding unnecessary regions of the protein structure. The prepared and optimized protein structure was then used for subsequent molecular docking studies of the synthesized compounds. In conclusion, proper preparation of the 7B6F protein ensures reliable docking simulations by maintaining structural integrity,[26] correct protonation states, and accurate representation of the binding site. This step is essential for identifying potential inhibitors and understanding ligand–protein interactions in Ovarian cancer drug discovery.

Preparation of ligand

For chemical structures, Chem Draw was used to sketch, which were then converted into three-dimensional structures. The ligands' overall energy-minimized Potential of stereoisomers were kept, and the refined ligands were stored in Maestro format. The derivatives of Imidazolidine ring and its substituted scaffolds with IUPAC names were used as ligands mention in Figure 2 for the docking study.

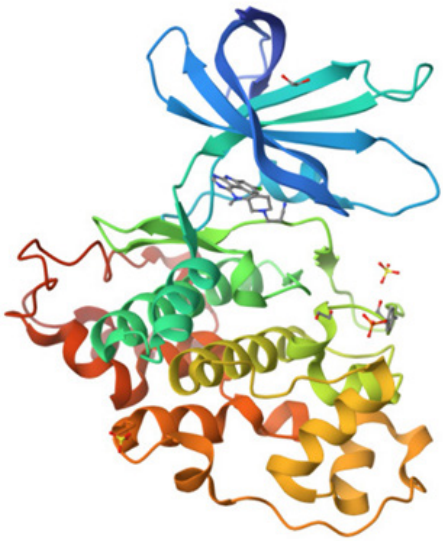


Fig. 1. Three-dimensional structure of the NUDT5 protein (PDB ID: 7B6F), illustrating the molecular target selected for computational investigation in the context of cancer-related drug discovery

RESULTS

Comparative Analysis of Physicochemical Properties

The physicochemical properties of the synthesized molecules (AM1–AM12) were systematically evaluated to determine their drug-likeness and suitability for further development. Key parameters, including rotatable bonds, hydrogen bond donors and acceptors, molar refractivity (MR), topological polar surface area (TPSA), and lipophilicity indices (iLOGP, XLOGP3, WLOGP, and MLOGP), were analyzed. The number of rotatable bonds ranged from 8 to 11, indicating moderate molecular flexibility among all compounds. Most molecules exhibited 8–9 rotatable bonds, suggesting a favorable balance between conformational adaptability and structural rigidity. However, AM10 showed the highest number of rotatable bonds (11), which may lead to increased flexibility and potentially reduced binding specificity. Hydrogen bonding capacity plays a crucial role in ligand–receptor interactions. The number of hydrogen bond acceptors ranged from 4 to 6, while hydrogen bond donors varied between 2 and 3. All compounds complied with Lipinski's rule of five, indicating good oral bioavailability potential. Notably, AM5 exhibited a slightly higher number of hydrogen bond donors, which may enhance binding interactions but could also reduce membrane permeability. Molar refractivity values ranged from 116.56 to 135.07, reflecting acceptable molecular volume and polarizability across all compounds. AM2 and AM6 showed the highest MR values, suggesting enhanced interaction potential due to increased polarizability, whereas AM7 displayed the lowest value, indicating a relatively smaller molecular size. The topological polar surface area (TPSA) values ranged from 65.96 to 111.78 Å². Compounds such as AM1, AM3, AM4, AM7, and AM9 exhibited TPSA values below 90 Å², indicating

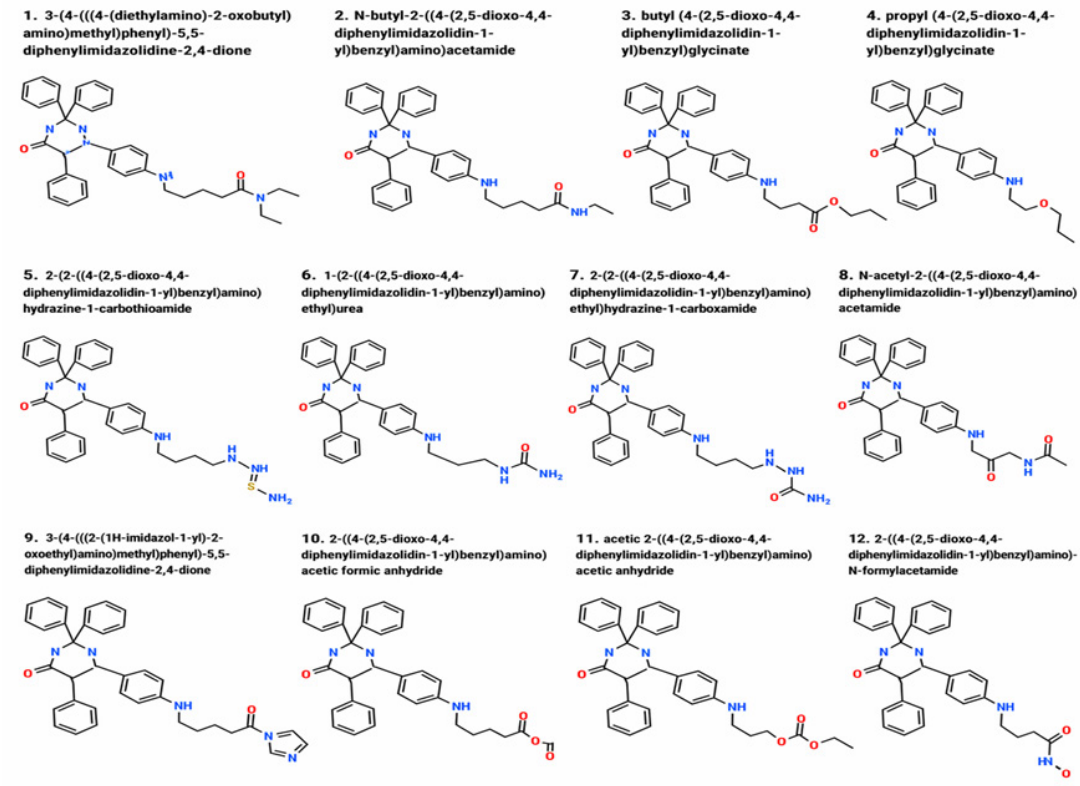


Fig. 2. Design strategy of the imidazolidine scaffold and its substituted derivatives investigated in the present study

good membrane permeability and potential for blood–brain barrier penetration. In contrast, AM2 and AM6 showed higher TPSA values (>100 Å²), which may limit their permeability. Lipophilicity is a critical determinant of drug absorption and distribution. The evaluated LogP values indicated that most compounds fall within the acceptable range. However, AM3 and AM4 exhibited relatively higher lipophilicity (XLOGP3 = 5.52), which may lead to poor aqueous solubility. On the other hand, AM10 showed lower lipophilicity, suggesting better solubility but possibly weaker membrane interaction. Compounds such as AM1, AM5, AM7, and AM9 demonstrated balanced lipophilicity, which is desirable for optimal pharmacokinetic behavior. All compounds satisfied Lipinski's rule of five, indicating favorable drug-like characteristics. Among the studied molecules, AM1, AM7, and AM9 demonstrated the most balanced physicochemical profiles, combining optimal lipophilicity, permeability, and molecular flexibility. In contrast, AM2 and AM6 may require structural optimization to improve permeability, while AM3 and AM4 may need modification to reduce excessive lipophilicity. In conclusion, the results suggest that AM1, AM7, and AM9 are promising lead candidates for further investigation, as they exhibit a favorable balance of physicochemical properties essential for drug development.

Comparative Analysis of ADMET Properties

The absorption, distribution, metabolism, and excretion (ADMET) profiles of the synthesized molecules (AM1–AM12) were evaluated to assess their pharmacokinetic behavior and potential suitability as drug candidates. Key parameters, including gastrointestinal (GI) absorption, blood–brain barrier (BBB) permeability, P-glycoprotein (P-gp) substrate specificity, cytochrome P450 (CYP) enzyme inhibition, and skin permeability (log Kp), were systematically analyzed. Comparative table containing GI absorption; BBB permeant; Pgp substrate; CYP1A2 inhibitor; CYP2C19 inhibitor; CYP2C9 inhibitor; CYP2D6 inhibitor; CYP3A4 inhibitor for AM1–AM12 was given in table 2. All compounds demonstrated high gastrointestinal (GI) absorption, indicating favorable oral bioavailability and efficient uptake within the gastrointestinal tract. This uniformity suggests that all molecules possess suitable physicochemical characteristics for oral administration. Blood–brain barrier permeability analysis revealed that AM1, AM3, AM4, AM7, and AM9 are predicted to be BBB permeant, suggesting their potential to penetrate the central nervous system (CNS). In contrast, AM2, AM5, AM6, AM8, and AM10 were predicted to be non-permeant, indicating limited CNS exposure. This distinction is particularly important depending on whether central or peripheral therapeutic activity is desired. The interaction with P-glycoprotein (P-gp), an important efflux transporter, showed that most compounds are non-substrates, except AM5, AM9, and AM10, which are predicted to be P-gp substrates. This suggests that these molecules may be subject to efflux, potentially reducing intracellular drug concentration and overall efficacy. Cytochrome P450 enzyme inhibition profiling indicated that none of the compounds inhibit CYP1A2, which is favorable as it reduces the likelihood of metabolic drug–drug interactions through this pathway. However, most compounds were predicted to inhibit multiple CYP isoforms, particularly CYP2C19, CYP2C9, and CYP3A4, which are key enzymes involved in drug metabolism. Notably, AM2 and AM6 did not inhibit CYP2D6, whereas the remaining compounds showed inhibitory activity toward this isoform. Interestingly, AM10 did not inhibit CYP2C19, distinguishing it from the other molecules. The broad CYP inhibition profile observed in most compounds may raise concerns regarding potential drug–drug interactions and metabolic liabilities. Skin permeability, represented by log Kp values, ranged from –5.13 to –6.7 cm/s, indicating generally low transdermal permeability for all compounds. Among them, AM3 and AM4 exhibited relatively higher permeability (–5.13 cm/s), while AM10 showed the lowest permeability (–6.7 cm/s), suggesting minimal dermal absorption. The ADMET analysis suggests that all compounds possess favorable oral absorption characteristics. Compounds AM1, AM3, AM4, and AM7 demonstrated a desirable balance of BBB permeability and non-substrate behavior toward P-gp, indicating efficient distribution potential. However, the widespread inhibition of CYP enzymes across most compounds highlights a need for careful optimization to minimize metabolic interactions. Additionally, compounds

Table 1. Comparative physicochemical properties of the designed imidazolidine derivatives (AM1–AM12), including the number of rotatable bonds, hydrogen-bond acceptors (HBA), hydrogen-bond donors (HBD), molar refractivity (MR), topological polar surface area (TPSA), and calculated lipophilicity parameters (iLOGP, XLOGP3, WLOGP, and MLOGP)

Comp. Code	#Rotatable bonds	#H-bond acceptors	#H-bond donors	MR	TPSA	iLOGP	XLOGP3	WLOGP	MLOGP
AM1	12	5	2	151.96	81.75	3.91	3.7	3.06	2.4
AM2	11	4	3	142.25	90.54	3.85	3.84	2.67	2.41
AM3	11	5	2	140.53	87.74	3.9	4.41	3.1	2.82
AM4	10	5	2	135.73	87.74	3.79	4.06	2.71	2.62
AM5	10	4	5	140.93	143.61	3.38	2.35	1.09	1.83
AM6	9	4	4	130.93	116.56	2.58	1.99	1.42	1.83
AM7	10	5	5	133.73	128.59	2.46	1.75	0.93	1.87
AM8	9	5	3	132.84	107.61	2.25	2.37	1.42	1.56
AM9	8	5	2	137.01	96.33	3	2.94	2.29	1.66
AM10	9	6	2	126.7	104.81	2.69	2.96	1.45	1.76
AM11	9	6	2	131.12	104.81	3.03	2.94	1.84	1.97
AM12	9	5	3	128.42	107.61	2.33	2.38	1.03	1.36

Table 2. Comparative predicted ADMET profiles of the designed imidazolidine derivatives (AM1–AM12), including gastrointestinal (GI) absorption, blood–brain barrier (BBB) permeability, P-glycoprotein (P-gp) substrate status, and predicted inhibitory interactions with cytochrome P450 (CYP) isoenzymes CYP1A2, CYP2C19, CYP2C9, CYP2D6, and CYP3A4

Comp. Code	GI absorption	BBB permeant	Pgp substrate	CYP1A2 inhibitor	CYP2C19 inhibitor	CYP2C9 inhibitor	CYP2D6 inhibitor	CYP3A4 inhibitor	log Kp (cm/s)
AM1	High	No	Yes	Yes	Yes	Yes	Yes	Yes	-6.71
AM2	High	No	Yes	Yes	Yes	Yes	Yes	Yes	-6.44
AM3	High	No	Yes	Yes	Yes	Yes	Yes	Yes	-6.05
AM4	High	No	Yes	No	Yes	Yes	Yes	Yes	-6.21
AM5	Low	No	Yes	No	No	No	Yes	No	-7.53
AM6	High	No	Yes	No	No	No	Yes	No	-7.59
AM7	High	No	Yes	No	No	No	No	No	-7.85
AM8	High	No	Yes	No	No	Yes	Yes	No	-7.4
AM9	High	No	Yes	No	Yes	Yes	Yes	Yes	-7.05
AM10	High	No	Yes	No	Yes	Yes	No	No	-6.9
AM11	High	No	Yes	No	Yes	Yes	Yes	Yes	-7
AM12	High	No	Yes	No	Yes	Yes	Yes	No	-7.31

such as AM5, AM9, and AM10 may require further modification to overcome P-gp-mediated efflux. In conclusion, AM1, AM3, AM4, and AM7 emerge as promising candidates based on their balanced ADMET profiles, while other compounds may require structural refinement to improve metabolic stability and reduce transporter-related limitations.

Comparative Analysis of Drug-Likeness and Bioavailability

The drug-likeness properties of the synthesized molecules (AM1–AM12) were evaluated using multiple established rules, including Lipinski, Ghose, Veber, Egan, and Muegge filters, along with bioavailability score assessment. Comparative table containing Lipinski #violations; Ghose #violations; Veber #violations; Egan #violations; Muegge #violations and Bioavailability Score for AM1–AM12 was given in table 3. These parameters are essential for predicting the suitability of compounds as orally active drug candidates. All the studied molecules exhibited zero violations of Lipinski's rule of five, indicating favorable physicochemical characteristics such as optimal molecular weight, lipophilicity, and hydrogen bonding capacity. This strongly suggests that all compounds possess good potential for oral bioavailability. The Ghose filter analysis revealed that most compounds complied with the criteria, except AM2, AM3, AM4, and AM6, each showing one violation. These deviations may be attributed to slight variations in molecular weight, molar refractivity, or logP values; however, a single violation is generally considered acceptable and does not significantly compromise drug-likeness. In terms of the Veber rule, which evaluates molecular flexibility and polar surface area, all compounds showed no violations except AM10, which exhibited one violation. This suggests that AM10 may have slightly reduced oral bioavailability due to increased flexibility or polar surface area. The Egan filter results indicated no violations across all compounds, supporting favorable passive membrane permeability and absorption characteristics. Similarly, the Muegge rule showed that most compounds comply well, with the exception of AM3 and AM4, each displaying one violation. These minor deviations suggest the need for slight structural optimization but do not significantly diminish their overall potential. The bioavailability score was consistent across all compounds, with a value of 0.55, indicating a moderate probability of oral bioavailability. This uniformity suggests that all molecules share comparable pharmacokinetic potential in terms of systemic availability. The analysis demonstrates that the majority of the compounds exhibit strong compliance with multiple drug-likeness filters, reinforcing their suitability as drug candidates. In particular, AM1, AM5, AM7, AM8, and AM9 showed no violations across all evaluated rules, indicating highly favorable drug-like characteristics. Compounds

Table 3. Comparative drug-likeness profiles of the designed imidazolidine derivatives (AM1–AM12), including the number of violations of Lipinski, Ghose, Veber, Egan, and Muegge criteria, together with the predicted bioavailability score

Comp. Code	Lipinski #violations	Ghose #violations	Veber #violations	Egan #violations	Muegge #violations	Bioavailability Score
AM1	0	3	1	0	0	0.55
AM2	0	1	1	0	0	0.55
AM3	0	1	1	0	0	0.55
AM4	0	1	0	0	0	0.55
AM5	0	1	1	1	0	0.55
AM6	0	1	0	0	0	0.55
AM7	0	1	0	0	0	0.55
AM8	0	1	0	0	0	0.55
AM9	0	1	0	0	0	0.55
AM10	0	0	0	0	0	0.55
AM11	0	1	0	0	0	0.55
AM12	0	0	0	0	0	0.55

AM2, AM3, AM4, and AM6 presented minor deviations in the Ghose and Muegge criteria, while AM10 showed a single violation in the Veber rule, suggesting a potential need for structural refinement. In conclusion, the findings highlight that most of the synthesized molecules possess desirable drug-likeness properties with minimal violations, supporting their further consideration in drug development studies. Among them, AM1, AM5, AM7, AM8, and AM9 emerge as the most promising candidates based on their complete compliance with all evaluated criteria.

Comparative Analysis of Molecular Docking and Binding Interactions

The molecular docking analysis of the synthesized derivatives (AM1–AM12) was performed to evaluate their binding affinity and interaction patterns within the active site of the target protein. The analysis included amino acid interactions, hydrophobicity profiles, pKa values, average isotropic displacement, and docking scores. All compounds demonstrated interactions with a highly conserved set of amino acid residues, including LYS36, VAL37, THR38, THR39, VAL40, VAL41, ALA42, THR43, PRO44, GLY45, GLN46, GLY47, PRO48, ASP49, and ARG50. The consistency of these interacting residues suggests that all derivatives bind within a similar active site region and follow a comparable binding mode. In the case of AM1, additional interactions extending up to residues such as GLN52, GLU53, VAL54, and SER55 were observed, indicating slightly enhanced binding coverage within the active pocket.

The hydrophobicity profile of interacting residues revealed a balanced distribution of hydrophobic and hydrophilic amino acids. Residues such as VAL37, VAL40, VAL41, and ALA42 contributed to hydrophobic interactions, while polar and charged residues including LYS36,

Table 4. Predicted molecular docking interactions of the designed imidazolidine derivatives (AM1–AM12) with the selected target protein (PDB ID: 7B6F), showing the interacting amino acid residues and corresponding ligand–protein interaction profiles.

Comp. Code	Name of Amino acid	Molecular Docking Score
AM-1	LYS36;VAL37;THR38;THR39;VAL40;VAL41;ALA42;THR43PRO44;GLY45; GLN46;GLY47;PRO48;ASP49;ARG50;PRO51GLN52;GLU53;VAL54;SER55	-7.7
AM -2	LYS36;VAL37;THR38;THR39;VAL40;VAL41;ALA42;THR43PRO44;GLY45; GLN46;GLY47;PRO48;ASP49;ARG50	-8.8
AM -3	LYS36;VAL37;THR38;THR39;VAL40;VAL41;ALA42;THR43PRO44;GLY45; GLN46;GLY47;PRO48;ASP49;ARG50	-7.1
AM -4	LYS36;VAL37;THR38;THR39;VAL40;VAL41;ALA42;THR43PRO44;GLY45; GLN46;GLY47;PRO48;ASP49;ARG50	-8.8
AM-5	LYS36;VAL37;THR38;THR39;VAL40;VAL41;ALA42;THR43PRO44;GLY45; GLN46;GLY47;PRO48;ASP49;ARG50	-9.4
AM -6	LYS36;VAL37;THR38;THR39;VAL40;VAL41;ALA42;THR43PRO44;GLY45; GLN46;GLY47;PRO48;ASP49;ARG50	-9.5
AM-7	LYS36;VAL37;THR38;THR39;VAL40;VAL41;ALA42;THR43PRO44;GLY45; GLN46;GLY47;PRO48;ASP49;ARG50	-9.5
AM -8	LYS36;VAL37;THR38;THR39;VAL40;VAL41;ALA42;THR43PRO44;GLY45; GLN46;GLY47;PRO48;ASP49;ARG50	-9.9
AM -09	LYS36;VAL37;THR38;THR39;VAL40;VAL41;ALA42;THR43PRO44;GLY45; GLN46;GLY47;PRO48;ASP49;ARG50	-9.6
AM -10	LYS36;VAL37;THR38;THR39;VAL40;VAL41;ALA42;THR43PRO44;GLY45; GLN46;GLY47;PRO48;ASP49;ARG50	-8.9
AM-11	LYS36;VAL37;THR38;THR39;VAL40;VAL41;ALA42;THR43PRO44;GLY45; GLN46;GLY47;PRO48;ASP49;ARG50	-6.8
AM -12	VAL37;THR38;THR39;VAL40;VAL41;ALA42;THR43PRO44;GLY45;GLN46; GLY47;PRO48;ASP49;ARG50	-9.9

ASP49, ARG50, and GLN46 facilitated hydrogen bonding and electrostatic interactions. This combination of interactions is crucial for stabilizing ligand–protein complexes and enhancing binding affinity. The pKa values of key residues, particularly lysine (10.4), arginine (12), and aspartic acid (3.9), indicate the presence of both acidic and basic environments within the binding pocket, which may support diverse interaction mechanisms such as ionic bonding and hydrogen bonding. The average isotropic displacement values ranged from approximately 35 to 83, suggesting moderate flexibility within the binding region, which may accommodate ligand binding without significant structural distortion. The docking scores ranged from –7.1 to –9.9 kcal/mol, indicating varying binding affinities among the compounds. Among all derivatives, AM8 exhibited the highest binding affinity (–9.9 kcal/mol), followed by AM9 (–9.6 kcal/mol), AM6 and AM7 (–9.5 kcal/mol each), and AM5 (–9.4 kcal/mol). These compounds demonstrate strong and stable interactions with the target protein. In contrast, AM3 showed the lowest binding affinity (–7.1 kcal/mol), indicating comparatively weaker interaction. AM1 also exhibited a relatively moderate docking score (–7.7 kcal/mol), despite interacting with a larger number of residues. Interestingly, compounds with stronger docking scores generally maintained consistent interaction patterns with key active site residues, suggesting that binding affinity is influenced more by interaction strength and orientation rather than the number of interacting residues alone. Additionally, the presence of both hydrophobic and polar interactions appears to play a significant role in enhancing docking performance. In conclusion, the molecular docking results indicate that AM8, AM9, AM6, and AM7 are the most promising candidates due to their superior binding affinities and stable interaction profiles. Compounds such as AM5 also demonstrate strong potential, while AM1 and AM3 may require structural optimization to improve their binding efficiency. Overall, the findings highlight the importance of balanced hydrophobic and electrostatic interactions in achieving optimal ligand–protein binding. Name of Amino acid, molecular docking of Design of imidazolidine and its substituted scaffolds by the targeted proteins was given in table 4.

DISCUSSION

The present study employed an integrated in silico approach to evaluate the therapeutic potential of designed imidazolidine derivatives (AM1–AM12) against the selected target protein (PDB ID: 7B6F). Molecular docking, physicochemical profiling, ADMET prediction, drug-likeness assessment, and structural interaction analysis were collectively used to prioritize compounds with favorable computational characteristics. The integration of these approaches provided a broader assessment of the designed derivatives; however, the findings should be interpreted within the limitations inherent to computational drug-discovery studies. Molecular docking analysis indicated that all compounds interacted within a well-defined active-site region involving conserved residues, including LYS36, VAL37, THR38, THR39, VAL40, ALA42, GLN46, ASP49, and ARG50. The recurrence of these residues across the ligand series suggested a broadly similar binding orientation. The calculated docking scores ranged from "7.1 to "9.9 kcal/mol, with AM8, AM9, AM6, and AM7 showing comparatively favorable predicted binding affinities. These results suggest that these compounds may have a higher propensity to interact with the target protein; however, docking scores should not be interpreted as direct evidence of biological potency or inhibitory activity. Docking algorithms provide an estimation of ligand–protein binding under defined computational conditions and may not fully account for protein flexibility, solvent effects, entropic contributions, induced-fit effects, or the dynamic nature of ligand binding. The predicted interactions involved a combination of hydrogen bonding, hydrophobic contacts, and electrostatic interactions. Hydrophobic residues such as VAL37, VAL40, and ALA42 appeared to contribute to non-polar contacts, whereas residues including LYS36, GLN46, ASP49, and ARG50 participated in polar or electrostatic interactions. The coexistence of hydrophilic and hydrophobic contacts may contribute to ligand stabilization within the predicted binding pocket. Nevertheless, the presence of a particular interaction in a docking pose does not necessarily confirm that the interaction is maintained under physiological conditions. Experimental structural studies or molecular dynamics simulations

would therefore be valuable for determining the persistence and stability of these interactions. The physicochemical evaluation showed that most derivatives exhibited properties compatible with commonly recognized drug-like chemical space. Parameters related to molecular flexibility, hydrogen-bonding capacity, molar refractivity, TPSA, and lipophilicity were generally within acceptable ranges. Compounds with relatively lower TPSA and balanced lipophilicity may have an improved probability of passive membrane diffusion. However, physicochemical descriptors alone cannot reliably predict cellular permeability, bioavailability, or tissue distribution. In particular, the predicted permeability of a compound may be influenced by factors such as transporter activity, membrane composition, ionization state, metabolism, and protein binding, which are not completely represented by conventional property-based assessments. ADMET prediction indicated high gastrointestinal absorption for all compounds, suggesting a potentially favorable oral absorption profile. However, these findings represent computational predictions rather than experimentally measured pharmacokinetic parameters. The observed differences in blood–brain barrier permeability may have therapeutic implications depending on the intended site of action, but BBB penetration should not automatically be regarded as beneficial. For an ovarian cancer-directed therapeutic, unnecessary central nervous system exposure could potentially increase the risk of off-target effects. Therefore, peripheral restriction may be advantageous for some candidates, whereas CNS penetration would only be desirable when supported by a specific therapeutic rationale. Most compounds were predicted to be non-substrates of P-glycoprotein, which may indicate a lower likelihood of transporter-mediated efflux. Nevertheless, these predictions cannot exclude transporter interactions in biological systems. Similarly, the predicted interactions with CYP enzymes, particularly CYP2C19, CYP2C9, and CYP3A4, should be considered cautiously. CYP inhibition may influence systemic exposure and could potentially result in drug–drug interactions. Therefore, the favorable ADMET profile predicted for the compounds should not be considered definitive evidence of pharmacokinetic safety. Experimental enzyme inhibition, microsomal stability, transporter studies, and animal pharmacokinetic investigations would be necessary to confirm these predictions. Drug-likeness analysis showed that most compounds complied with Lipinski, Veber, and Egan criteria, with only minor deviations observed for selected derivatives. These results support their compatibility with commonly used oral drug-development guidelines. However, compliance with drug-likeness rules does not guarantee efficacy, safety, adequate exposure, or clinical developability. Such rules are primarily filtering tools and should therefore be used in combination with biological, pharmacokinetic, and toxicological evidence rather than as independent indicators of therapeutic success. When the overall computational findings were considered collectively, AM1, AM3, AM4, and AM7 demonstrated a favorable balance of physicochemical and pharmacokinetic characteristics, whereas AM8 and AM9 showed superior predicted docking performance. AM7 was particularly notable because of its comparatively balanced binding, ADMET, and drug-likeness characteristics. Thus, AM7, AM8, and AM9 may be considered prioritized candidates for subsequent investigation. Importantly, the ranking of these compounds depends on the weighting of different computational parameters; a compound with the strongest docking score may not necessarily represent the most suitable lead when pharmacokinetic, toxicity, synthetic accessibility, and selectivity characteristics are considered simultaneously. This provides an alternative interpretation of the present findings and emphasizes that lead selection should not rely solely on docking affinity.

CONCLUSION

The present in silico investigation provided a computational assessment of imidazolidine derivatives (AM1–AM12) against the selected protein target (PDB ID: 7B6F) using molecular docking, physicochemical profiling, ADMET prediction, drug-likeness evaluation, and structural interaction analysis. The docking results showed that AM8, AM9, AM6, and AM7 exhibited comparatively favorable predicted binding affinities, with interactions involving key residues within the target binding site. Among

the evaluated compounds, AM1, AM3, AM4, and AM7 demonstrated relatively balanced physicochemical and predicted pharmacokinetic characteristics, while AM7 showed an overall favorable computational profile when the different parameters were considered collectively. Based on the integrated computational findings, AM7, AM8, and AM9 can be prioritized as lead candidates for further investigation, rather than being considered confirmed therapeutic agents. The present results provide a rational basis for further structural optimization and experimental evaluation of the imidazolidine scaffold. However, the predicted docking affinities, ADMET characteristics, and drug-likeness properties cannot establish anticancer efficacy, target inhibition, or clinical safety. Therefore, the therapeutic relevance of these compounds remains to be determined through appropriate experimental studies. Future investigations should include molecular dynamics and binding free-energy studies to further examine ligand–protein interaction stability, followed by in vitro target-inhibition and cytotoxicity studies, selectivity assessment, metabolic stability and CYP-enzyme evaluation, and appropriate in vivo pharmacokinetic and efficacy studies. Such investigations will be essential to determine whether the favorable computational characteristics identified in the present study translate into reproducible biological activity and to establish the suitability of the selected derivatives as potential leads for further anticancer drug-discovery research.

ACKNOWLEDGEMENT

The authors are thankful to Pravara Rural College of Pharmacy, Pravaranagar.

Funding Sources

The author(s) received no financial support for the research, authorship, and/or publication of this article.

Conflict of interest

The authors do not have any conflict of interest.

Data Availability Statement

This statement does not apply to this article.

Ethics Statement

This research did not involve human participants, animal subjects, or any material that requires ethical approval.

Informed Consent Statement

This study did not involve human participants, and therefore, informed consent was not required.

Clinical Trial Registration

This research does not involve any clinical trials.

Permission to reproduce material from other sources

Not Applicable.

Author Contributions

Harshada Subhash Bhosale: Collection and analysis of in silico ADMET data; Ashok Yuvraj Dalimbe: Drafting the original manuscript; Sachin Dattatraya Nawale: Data interpretation and scientific writing; Pranali Satish Pandarkar: Introduction and literature background; Rohit Jaysing Bhor: Design and structural drawing of synthesized drug derivatives; Divya Ravindra Shivtare: Data organization, and critical revision of the manuscript; Aditya Anil Pachpute: Critical revision of the manuscript for intellectual content.

REFERENCES

1. Alam MS, Choudhury S, Rahman MM. Advances in molecular docking and structure-based drug design. *Curr Top Med Chem.* 2021;21(18):1674-1692. doi:10.2174/1568026621666210616112435
2. Baell JB, Nissink JWM. Seven year itch: pan-assay interference compounds (PAINS) in 2020. *J Med Chem.* 2020;63(16):8408-8421. doi:10.1021/acs.jmedchem.9b01982
3. Bender A, Cortés-Ciriano I. Artificial intelligence in drug discovery: what is realistic, what are illusions? *Nat Rev Drug Discov.* 2021;20(5):353-364. doi:10.1038/s41573-021-00173-3
4. Berman HM, Westbrook J, Feng Z, et al. The Protein Data Bank. *Nucleic Acids Res.* 2000;28(1):235-242. doi:10.1093/nar/28.1.235
5. Daina A, Michielin O, Zoete V. SwissADME: a free web tool to evaluate pharmacokinetics, drug-likeness and medicinal chemistry friendliness of small molecules. *Sci Rep.* 2017;7:42717. doi:10.1038/srep42717
6. DiMasi JA, Grabowski HG, Hansen RW. Innovation in the pharmaceutical industry: new estimates of R&D costs. *J Health Econ.* 2016;47:20-33. doi:10.1016/j.jhealeco.2016.01.012

7. Ferreira LG, Dos Santos RN, Oliva G, Andricopulo AD. Molecular docking and structure-based drug design strategies. *Molecules.* 2015;20(7):13384-13421. doi:10.3390/molecules200713384
8. Ferreira RS, Simeonov A, Jadhav A, et al. Complementarity between docking and high-throughput screening in drug discovery. *J Med Chem.* 2020;63(9):4255-4272. doi:10.1021/acs.jmedchem.9b01989
9. Ghose AK, Viswanadhan VN, Wendoloski JJ. A knowledge-based approach in designing combinatorial or medicinal chemistry libraries for drug discovery. *J Comb Chem.* 1999;1(1):55-68. doi:10.1021/cc9800071
10. Gorgulla C, Boeszoermenyi A, Wang ZF, et al. An open-source drug discovery platform enables ultra-large virtual screens. *Nat Methods.* 2020;17(10):1034-1037. doi:10.1038/s41592-020-0935-x
11. Hughes JP, Rees S, Kalindjian SB, Philpott KL. Principles of early drug discovery. *Br J Pharmacol.* 2011;162(6):1239-1249. doi:10.1111/j.1476-5381.2010.01127.x
12. Jorgensen WL. Efficient drug lead discovery and optimization. *Acc Chem Res.* 2009;42(6):724-733. doi:10.1021/ar800236t
13. Jumper J, Evans R, Pritzel A, et al. Highly accurate protein structure prediction with AlphaFold. *Nature.* 2021;596(7873):583-589. doi:10.1038/s41586-021-03819-2
14. Kirchmair J, Markt P, Distinto S, et al. Evaluation of the performance of 3D virtual screening protocols. *J Chem Inf Model.* 2008;48(4):834-844. doi:10.1021/ci700457y
15. Kitchen DB, Decornez H, Furr JR, Bajorath J. Docking and scoring in virtual screening for drug discovery: methods and applications. *Nat Rev Drug Discov.* 2004;3(11):935-949. doi:10.1038/nrd1549
16. Lavecchia A. Deep learning in drug discovery: opportunities, challenges and future prospects. *Drug Discov Today.* 2021;26(3):617-627. doi:10.1016/j.drudis.2020.11.003
17. Lipinski CA. Lead- and drug-like compounds: the rule-of-five revolution. *Drug Discov Today Technol.* 2004;9(8):337-341. doi:10.1016/S1359-6446(03)03003-6
18. Lipinski CA, Lombardo F, Dominy BW, Feeney PJ. Experimental and computational approaches to estimate solubility and permeability in drug discovery. *Adv Drug Deliv Rev.* 2001;46(1-3):3-26. doi:10.1016/S0169-409X(00)00129-0
19. Lionta E, Spyrou G, Vassilatis DK, Cournia Z. Structure-based virtual screening for drug discovery: principles, applications and recent advances. *Curr Top Med Chem.* 2014;14(16):1923-1938. doi:10.2174/1568026614666140929124445
20. Macarron R, Banks MN, Bojanic D, et al. Impact of high-throughput screening in biomedical research. *Nat Rev Drug Discov.* 2011;10(3):188-195. doi:10.1038/nrd3368
21. Meng XY, Zhang HX, Mezei M, Cui M. Molecular docking: a powerful approach for structure-based drug discovery. *Curr Comput Aided Drug Des.* 2011;7(2):146-157. doi:10.2174/157340911795677602
22. Morris GM, Huey R, Lindstrom W, et al. AutoDock4 and AutoDockTools4: automated docking with selective receptor flexibility. *J Comput Chem.* 2009;30(16):2785-2791. doi:10.1002/jcc.21256
23. Nuti R, Orioli E, Nencetti S. NUDT5: a new perspective in cancer therapy. *J Enzyme Inhib Med Chem.* 2019;34(1):130-138. doi:10.1080/14756366.2018.1545762
24. O'Boyle NM, Banck M, James CA, et al. Open Babel: an open chemical toolbox. *J Cheminform.* 2011;3:33. doi:10.1186/1758-2946-3-33
25. Pires DEV, Blundell TL, Ascher DB. pkCSM: predicting small-molecule pharmacokinetic and toxicity properties. *J Med Chem.* 2015;58(9):4066-4072. doi:10.1021/acs.jmedchem.5b00104
26. Pushpakom S, Iorio F, Eyers PA, et al. Drug repurposing: progress, challenges and recommendations. *Nat Rev Drug Discov.* 2020;19(8):511-530. doi:10.1038/s41573-019-0040-z